PAPER

Memristive synaptic device based on a natural organic material—honey for spiking neural network in biodegradable neuromorphic systems

To cite this article: Brandon Sueoka and Feng Zhao 2022 *J. Phys. D: Appl. Phys.* **55** 225105

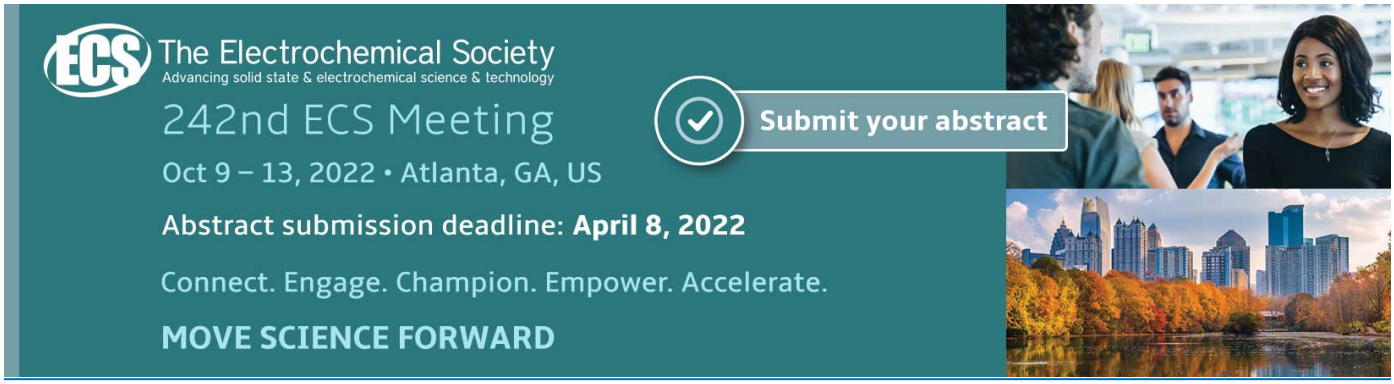

IOP Publishing Journal of Physics D: Applied Physics
J. Phys. D: Appl. Phys. **55** (2022) 225105 (7pp) https://doi.org/10.1088/1361-6463/ac585b

Memristive synaptic device based on a natural organic material—honey for spiking neural network in biodegradable neuromorphic systems

Brandon Sueoka and Feng Zhao*

Micro/Nanoelectronic and Energy Laboratory, School of Engineering and Computer Science, Washington State University, Vancouver, WA 98686, United States of America

E-mail: feng.zhao@wsu.edu

Received 4 January 2022, revised 17 February 2022
Accepted for publication 24 February 2022
Published 7 March 2022

Abstract

Spiking neural network (SNN) in future neuromorphic architectures requires hardware devices to be not only capable of emulating fundamental functionalities of biological synapse such as spike-timing dependent plasticity (STDP) and spike-rate dependent plasticity (SRDP), but also biodegradable to address current ecological challenges of electronic waste. Among different device technologies and materials, memristive synaptic devices based on natural organic materials have emerged as the favourable candidate to meet these demands. The metal–insulator-metal structure is analogous to biological synapse with low power consumption, fast switching speed and simulation of synaptic plasticity, while natural organic materials are water soluble, renewable and environmental friendly. In this study, the potential of a natural organic material—honey-based memristor for SNNs was demonstrated. The device exhibited forming-free bipolar resistive switching, a high switching speed of 100 ns set time and 500 ns reset time, STDP and SRDP learning behaviours, and dissolving in water. The intuitive conduction models for STDP and SRDP were proposed. These results testified that honey-based memristive synaptic devices are promising for SNN implementation in green electronics and biodegradable neuromorphic systems.

Keywords: spiking neural network, neuromorphic systems, memristor, biodegradable, spike-timing dependent plasticity, spike-rate dependent plasticity, natural organic material

(Some figures may appear in colour only in the online journal)

1. Introduction

High energy efficiency of biological nervous systems drives the development of spiking neural networks (SNNs) which offer more energy efficient deep learning. However, one challenge for SNN implementation in future neuromorphic systems is the demand of hardware, i.e. artificial synaptic devices which are the building block of SNNs, with not only the functionality of emulating biological synapses and realizing fundamental synaptic plasticity such as spike-timing dependent plasticity (STDP) and spike-rate dependent plasticity (SRDP), but also biodegradability to address current ecological challenges of electronic waste. STDP and SRDP play the most important roles in the development and refinement of neuronal circuits during brain development [1–3]. They are responsible for learning processes in the brain and retaining new information in neurons, and serve as the synaptic weight modification

* Author to whom any correspondence should be addressed.

rule for SNNs [4] via learning protocols, for example, the famous Hebbian learning rule that 'those who fire together, wire together' [5]. Technologies including two terminal memristors and three-terminal transistors based on inorganic, polymer and natural organic materials have been proposed for artificial synaptic devices [6–15]. Among them, memristive devices based on natural organic materials such as protein and polysaccharide have inspired research interest due to their high storage density, fast switching speed, low power consumption and analog to biological synapse while combined with the advantages of biodegradable, environmentally friendly, renewable and abundant in nature.

In our recent work, we have developed memristors based on honey, a natural material containing mainly monosaccharides, disaccharides and trisaccharides. These honey-based memristive devices successfully demonstrated [16, 17] bipolar resistive switching characteristics and imitated synaptic plasticities such as synaptic potentiation and depression, short-term and long-term memory, spatial summation and shunting inhibition, paired-pulse facilitation, high-pass synaptic filtering. In this study, honey-based memristor was fabricated and their switching speed, STDP and SRDP learning behaviours, and solubility in water were characterized for the first time. The intuitive conduction models for STDP and SRDP were proposed. Our work laid a foundation for making use of natural organic materials based artificial synaptic devices for green electronics and implementation of SNNs in biodegradable neuromorphic systems.

2. Experimental

The honey based memristors were fabricated by a bottom-up process into a metal–insulator-metal (MIM) structure with dried honey film as the resistive switching layer. Schematic of the process flow is shown in figure 1(a). A 2.5 × 2.5 cm^2 glass slide was used as a substrate and cleaned in an ultrasonic bath by acetone, isopropyl alcohol and deionized (D.I.). water for 10 min in each solution. A 200 nm thick Cu film was deposited by sputtering on the glass slide and used as the bottom electrode. Commercial honey was mixed carefully with D.I. water for a 30% concentration by weight till no visible honey crystals in the final honey solution, and then stored in a vacuum desiccator for 1 h to remove air bubbles. The honey solution was spin-coated on the Cu/glass substrate at 1000 rpm for 90 s, followed by baking on a hotplate at 90 °C for 9 h in air. After baking, a part of the Cu film was oxidized into Cu_xO. Our previous study [17] showed that the thickness of the dried honey film after this spin rate and baking temperature/time was about 2.5 μm. Finally, an array of 200 nm thick Cu top electrodes with circular patterns of 200 μm diameters was deposited by sputtering on the honey film through a stencil mask to complete the fabrication of Cu/honey/Cu_xO memristor devices.

All electrical tests were performed on a probe-station at room temperature in air. Resistive switching was measured with voltage sweep applied on the Cu top electrode and ground on the bottom Cu_xO electrode using a semiconductor

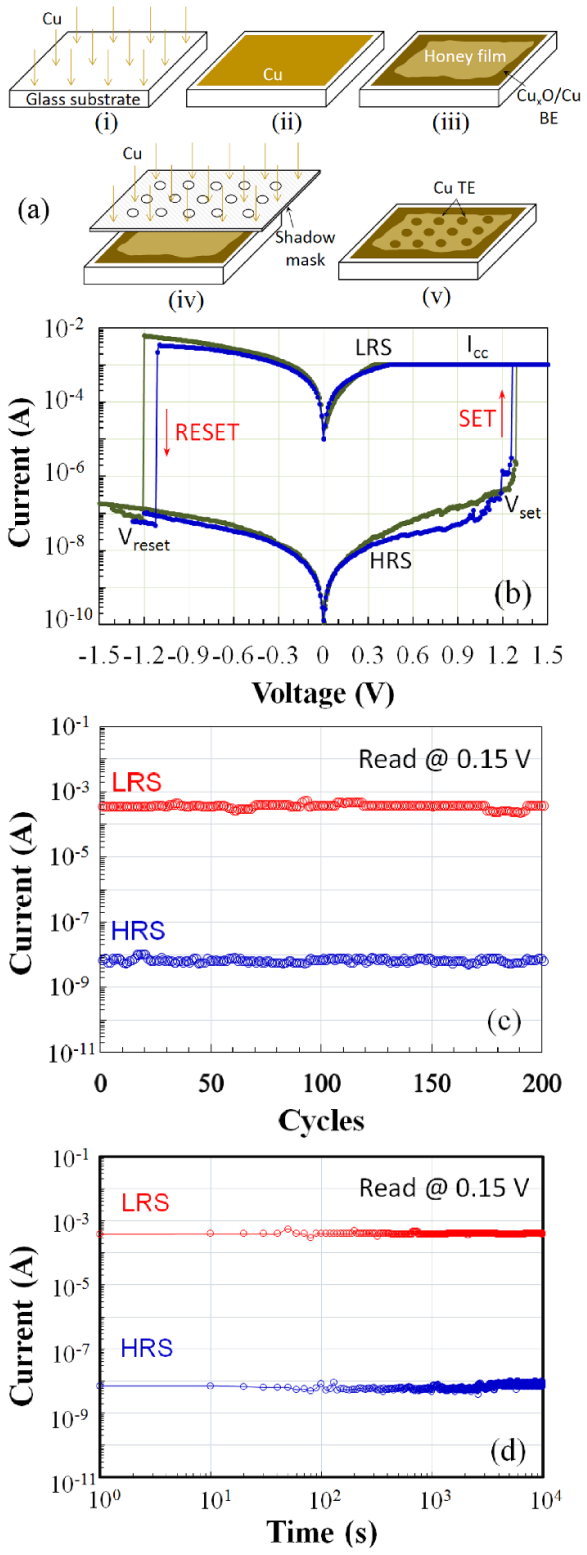

Figure 1. (a) Schematic of process flow for Cu/honey/Cu_xO memristor: (i) deposition of Cu on glass substrate, (ii) after Cu deposition, (iii) formation of honey film and Cu_xO/Cu BE, (iv) deposition of Cu TE through a shadow mask, (v) finished device. (b) Bipolar resistive switching characteristics. I_{CC}: current compliance to protect device from breakdown in the SET process. (c) Endurance test in a DC switching sweep mode at a read voltage of 0.15 V. (d) Retention tests under a continuous read voltage stress of 0.15 V.

characterization system. Transient, STDP and SRDP behaviours were characterized with voltage pulses applied by an arbitrary function generator and measured by an oscilloscope. In STDP measurements, identical rectangular-shaped voltage pulses (±0.8 V, 20 ms) with different time intervals of 20 ms, 25 ms, 30 ms, 35 ms, 40 ms, 100 ms, 150 ms and 200 ms were applied on the top Cu electrode and bottom Cu_xO electrode. In SRDP measurements, voltage spike trains with 30 repetitive pulses (1 V, 20 ms) and different frequencies of 0.5 Hz and 25 Hz were applied on the top Cu electrode to compare the current response.

3. Results and discussions

Resistive switching behaviours of the Cu/honey/Cu_xO memristor were characterized with typical *I–V* curves shown in figure 1(b). The device exhibited bipolar resistive switching characteristics with positive SET (V_{set}) voltage and negative RESET voltage (V_{reset}), but without forming process. These behaviours are consistent with our previously reported [16] results. The V_{reset} is similar, 1.1 V vs 1 V, while V_{set} is slightly smaller, 1.2 V vs 1.8 V. This result translates to a smaller read memory window but at the same time a much lower operation power. The endurance cycling test results by repetitive sweeping operation at a read voltage of 0.15 V are shown in figure 1(c). In 200 endurance cycles, the memristor retained conductance and reproduced resistive switching without significant current change in both high resistance state (HRS) and low resistance state (LRS). The retention was conducted to evaluate the non-volatile property as shown in figure 1(d) using 0.15 V as the read voltage. The memristor showed good retention characteristics up to 10^4 s without serious degradation in both HRS and LRS.

The schematic circuit diagram for characterization of the switching speed of Cu/honey/Cu_xO memristor is shown in figure 2(a). A load resistor R_L of 100 Ω was connected in series with the device as a voltage divider and current limiter. The device was triggered in pulse mode [18] to test resistive switching in a short timescale. The input SET and RESET voltage pulses (+3.2 V/5 μs and −1.6 V/5 μs) were applied with output voltage pulse on the Cu/honey/Cu_xO memristor measured. Current in the device was calculated by the voltage drop on the load resistor. Transient responses of resistive switching in SET and RESET process are illustrated in figures 2(b) and (c), with the switching speed defined by the SET and RESET time. The SET time is defined by the time it takes for device to transit from HRS to LRS in the SET process, which is characterized by the time delay between input and output voltage pulses. The RESET time is determined by the time for device to transit from LRS to HRS in the RESET process, which is demonstrated by the pulse width of the output voltage pulse. As shown in figures 2(b) and (c), the SET and RESET time were 100 ns and 500 ns, respectively. Such switching speed is comparable to other reported memristors such as Ag/pectin/indium tin oxide (ITO) [19] and emerging metal oxide [20, 21] resistive switching memories.

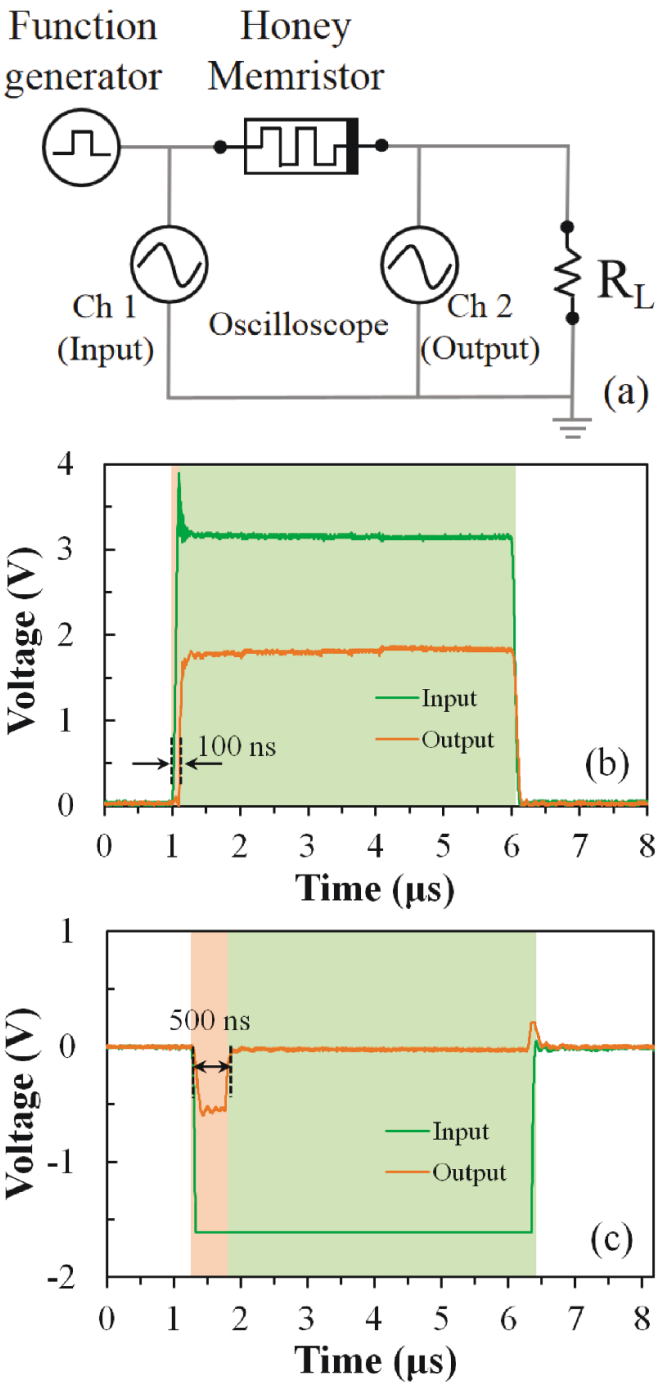

Figure 2. (a) Schematic diagram of the test setup for switching speed measurement. Transient response in (b) SET and (c) RESET process with Cu/honey/Cu_xO memristor triggered by input voltage pulse. The SET and RESET time was extracted from the delay time and output voltage pulse width, respectively.

As shown in figure 3(a), Cu/honey/Cu_xO memristor has a metal–insulator-metal (MIM) structure which resembles the biological synapse, with the top Cu electrode analogous to the axon terminal of the pre-neuron, the bottom Cu_xO electrode to the dendritic spine of the post-neuron and the honey film to the synapse cleft. The STDP process is

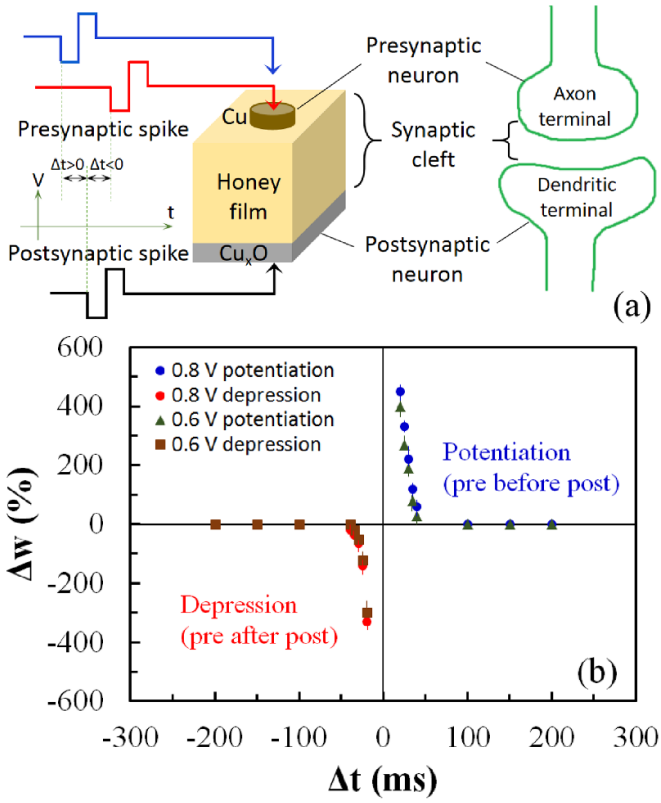

Figure 3. STDP learning implementation in Cu/honey/Cu$_x$O memristor. (a) Schematic diagram of Cu/honey/Cu$_x$O memristor analogous to a biological synapse, with synaptic action potentials mimicked by voltage pulses applied on the electrodes. Presynaptic pulse is before (blue) or after (red) postsynaptic pulse. (b) Change of synaptic weight Δw with relative timing Δt of the presynaptic and postsynaptic pulse to demonstrate potentiation and depression effect. Six devices were tested under 0.8 V and 0.6 V peak voltages, with maximum, minimum and average Δw plotted.

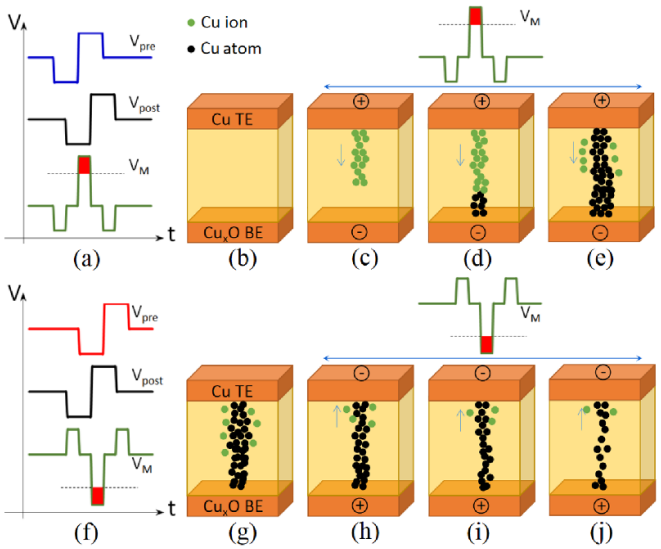

Figure 4. Schematic voltage waveforms and intuitive conduction models for STDP of Cu/honey/Cu$_x$O memristor. (a) Positive Δt when presynaptic voltage pulse V_{pre} is ahead of postsynaptic voltage pulse V_{post}, and voltage pulse on the memristor V_M is the difference between V_{pre} and V_{post}, $V_M = V_{pre} - V_{post}$. (b) Initial state of the memristor in off-state. (c)–(e) Redox of Cu ions and atoms in the honey film and conductive path formed by Cu filaments under positive V_M. (f) Negative Δt when presynaptic voltage pulse V_{pre} is behind postsynaptic voltage pulse V_{post}, with $V_M = V_{pre} - V_{post}$. (g) Initial state of the memristor in on-state. (h)–(j) Rupture of Cu filaments to breakdown the conductive path under negative V_M. The red area in V_M contributes to the change in synaptic strength. The arrows indicate the draft direction of Cu ions under electric field.

closely correlated with the relative timing of action potentials (or spikes) of pre- and postsynaptic neurons. The synaptic weight increases or decreases when the presynaptic spike reaches the synapse a few milliseconds before or after the postsynaptic spikes, which strengthens or weakens the synaptic connection and leads to potentiation or depression of the synapse, respectively. In STDP measurement, identical rectangular-shaped voltage pulses (±0.8 V, 20 ms) with different time intervals were applied on the top Cu electrode and bottom Cu$_x$O electrode to emulate pre- and postsynaptic spikes respectively and modulate conductance of the honey film. Excitatory postsynaptic current and synaptic weight were mimicked by the current in the Cu/honey/Cu$_x$O memristor. The change of the synaptic weight Δw is defined by $\Delta w = (I_{after} - I_{before})/I_{before} \times 100\% = (G_{after} - G_{before})/G_{before} \times 100\%$ [22], where I_{before} and I_{after} are currents and G_{before} and G_{after} are conductance in the memristor before and after pre- and postsynaptic voltage pulses (V_{pre} and V_{post}) were applied. A total of six devices were tested under 0.8 V and 0.6 V peak voltages, with the maximum, minimum and average Δw plotted as a function of the relative timing Δt of the applied voltage pulses shown in figure 3(b). $\Delta t = t_{post} - t_{pre}$ is the time interval between the beginning of the postsynaptic spike and the beginning of the presynaptic spike. Δt is positive (negative) when voltage pulse on the top Cu electrode is ahead (behind) of the voltage pulse on the bottom Cu$_x$O electrode. Results in figure 3(b) showed potentiation and depression behaviours, and with the decrease of the relative time Δt between V_{pre} and V_{post}, potentiation and depression effects were enhanced. These characteristics agree with STDP in biological synapses. Due to the digital switching nature of Cu/honey/Cu$_x$O memristor as shown in figure 1(b), the pulsing voltage was limited. Above a 0.8 V peak voltage no STDP characteristics were obtained from the devices. Our recent study found that the top electrode metals play a critical role to achieve digital and analog switching. With analog switching, a larger range of pulsing voltages can be applied. A comprehensive study on the effect of peak voltage and time interval on different devices with analog switching is under investigation.

Figure 4 depicts the schematic voltage waveforms and intuitive conduction models for STDP of the Cu/honey/Cu$_x$O memristor. The presynaptic voltage—and postsynaptic voltage pulses (±0.8 V, 20 ms) were designed so that each single pulse could not affect the memristor's conductance. When they overlapped, a voltage drop on the memristor, $V_M = V_{pre} - V_{post}$, was generated with the amplitude sufficiently large to modulate the memristor's conductance. As shown in figure 4(a), when V_{pre} was before V_{post}, V_M was

positive, with amplitude larger than V_{set}. As discussed in our previous study [16], with such positive voltage on the top Cu electrode, Cu electrode was oxidized into Cu cations (Cu^{+} and Cu^{2+}) which diffused into the honey film and drifted toward the bottom Cu_xO electrode under the electric field (figure 4(c)). When arriving at the Cu_xO surface, Cu cations were reduced back to Cu atoms and nucleate on the Cu_xO surface (figure 4(d)). This process continued and Cu atoms accumulated and self-assembled into Cu filaments to form a metallic path (figure 4(e)) which reduced the memristor's conductance and led to synaptic potentiation. As shown in figure 4(f), when V_{pre} was after V_{post}, V_M was negative, with amplitude larger than V_{reset}. With this negative voltage pulse applied on the top Cu electrode, Cu cations moved toward the top Cu electrode to reduce to Cu atoms and assembled back on the Cu surface, and the faradaic current and joule heating gradually dissolved Cu filaments in the initial state of the memristor (figure 4(g)) and ruptured the conductive path [16], as in figures 4(h)–(j), which increased the memristor's conductance and led to synaptic depression. Furthermore, with the decrease of the relative time Δt between V_{pre} and V_{post} till the pulse width of 20 ms, the overlapped (red) area in V_M increased and it increased the formation (when positive) or rupture (when negative) of the conductive path and therefore enhanced potentiation and depression effect, as shown by the change of Δw with Δt in figure 3(b).

SRDP is another important synaptic learning function in human neural networks especially for brain cognitive behaviours [23, 24]. In SRDP process, the synaptic weight is frequency dependent since it is modulated according to the firing frequency (rate) of presynaptic spikes between neurons. A higher rate or frequency leads to synaptic potentiation and memory effects. Unlike STDP test in which stimulation was applied on both top and bottom electrodes (pre- and post-synaptic neurons), voltage pulses in SRDP test were applied only on the top Cu electrode (presynaptic neuron) to mimic presynaptic spikes with current response in the memristor emulating the synaptic weight. The time-dependent current response of Cu/honey/Cu_xO memristor is shown in figure 5(a) when a positive voltage spike train (amplitude: 1 V, frequency: 0.5 Hz, pulse width: 20 ms) with 30 repetitive stimulation pulses was applied on the top Cu electrode. The current decayed instantaneously after each stimulation pulse, indicating that no potentiation occurred. When stimulus frequency of the voltage spike train increased to 25 Hz, as shown in figure 5(b), it was observed that the magnitude of the currents increased, indicating a synaptic potentiation with increased synaptic weight. Following the positive voltage spike train, a negative voltage spike train of 30 repetitive pulses (amplitude: −0.8 V, frequency: 0.5 Hz, pulse width: 20 ms) was applied to modulate the synaptic weight of the honey memristor. The obtained currents demonstrated synaptic depression behaviour by magnitude of currents decreasing. As shown in figure 5(d), when stimulation pulse with low frequency was applied on the memristor, only weak and instable conductive path by Cu filaments was formed in the honey film, therefore the conductance was lower and memristor relaxed back to its initial off-state after voltage pulse. When consecutive

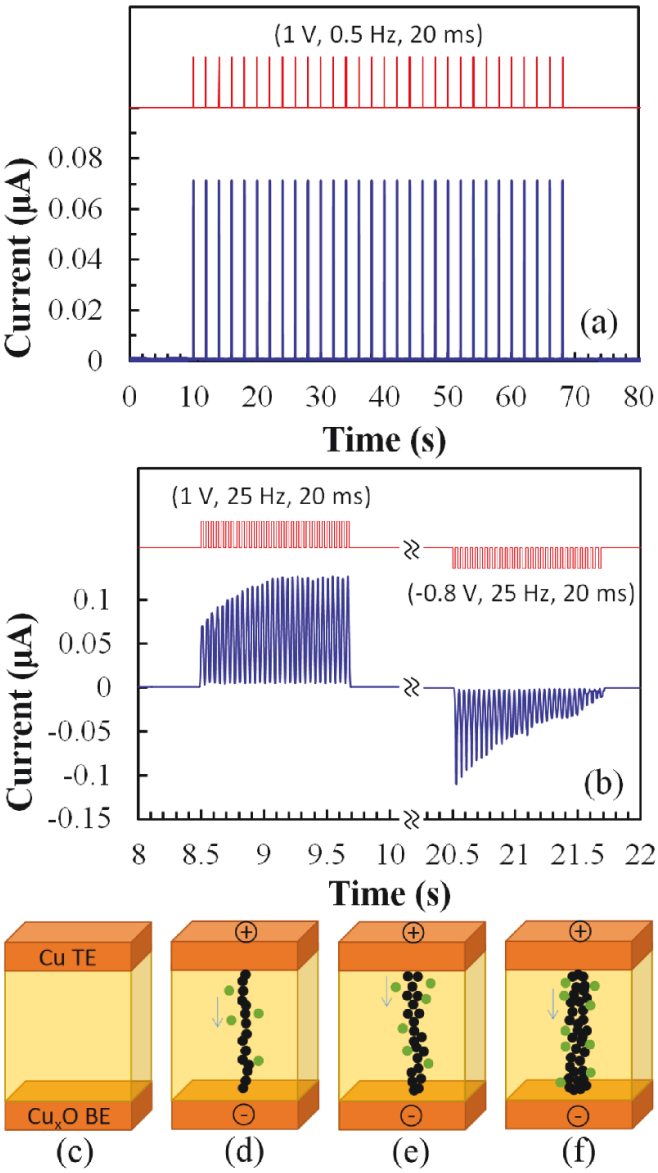

Figure 5. SRDP learning implementation in Cu/honey/Cu_xO memristor and intuitive conduction models. (a) Current response (blue) showed no potentiation when the frequency of the presynaptic spike train (red) was 0.5 Hz. (b) Synaptic potentiation and depression occurred when frequency increased to 25 Hz, indicating that the synaptic weight is frequency or rate dependent. (c) Initial state of the memristor in off-state. (d) Weak Cu filaments formed by single voltage spike. (e), (f) Extended Cu filaments formed by consecutive voltage spikes.

voltage pulses in the spike train with a higher frequency were applied, extended Cu filaments were formed (figures 5(e) and (f)), which resulted in increased conductance of the honey film and therefore an increased current. Biological synaptic spikes between neurons are at frequencies of 1–10 Hz [25]. Our tested STDP and SRDP functions with inherent self-adaption behaviours to relative timing and firing frequency testified that the time and frequency required for spikes are not a limitation, indicating the potential of honey-based memristor for spike neural network and neuromorphic system with a higher frequency than the biological systems. Recently a new hybrid

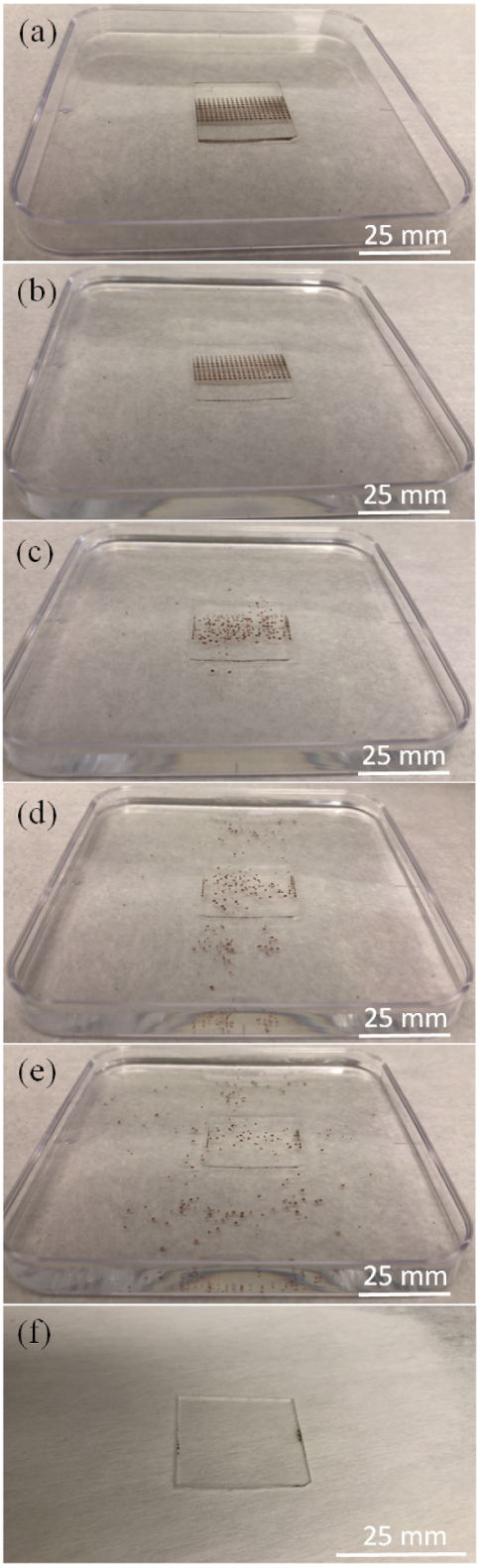

Figure 6. Photographs showing dissolution of honey and lift-off of Cu top electrodes in D.I. water at room temperature. Agitation was applied by shaking the container and water to speed up the dissolution process. (a) Initial sample after fabrication. After immersed in D.I. water for (b) 0 min, (c) 1 min, (d) 2 min, (e) 3 min and (f) after honey completely dissolved and sample was taken out of D.I. water and dried by nitrogen gas flow.

CMOS-memristive circuit [26, 27] was proposed to emulate a number of biological synaptic functions including STDP and SRDP and generate BCM-like behaviours. In our future work, we will perform experiment on honey-based memristor using the hybrid circuit to realize SRDP for showing the BCM rule.

One of the advantages of natural organic materials based memristor is the degradability over time due to their solubility in water, which makes them environmentally friendly. The dissolution experiment was carried out by immersing Cu/honey/glass in D.I. water at room temperature. In order to clearly show honey dissolution process and improve the contrast of the top circular Cu electrodes, the sample has no bottom Cu_xO film. A set of evolution images was collected during dissolution process and shown in figure 6. The honey active switching layer was fully dissolved by reacting with water even though it experienced a 9 h baking at 90 °C when forming the honey film. Since Cu also does not dissolve in water, Cu top electrodes were lifted off from the sample indicating that the honey film dissolved in water. For honey-based memristor to be used in green electronics and degradable neuromorphic systems, Cu electrodes need to be replaced by other dissolvable metals such as Mg or W [28, 29]. The resistive switching and synaptic behaviours of Mg/honey/Mg memristors are under investigation.

In this study, the mechanisms responsible for STDP and SRDP were proposed by only considering the redox of Cu top electrode and Cu filament formation and rupture, without the potential contribution from Cu_xO in the bottom electrode. Recently we have also fabricated honey-based memristor on ITO bottom electrode [17] with demonstration of memristive characteristics and synaptic behaviours. The results indicate that honey is an active resistive switching layer. However, it has been reported [30] that Cu_xO is also an effective resistive switching material therefore it could also contribute to the resistive switching and synaptic properties when it is a part of the bottom electrode in the honey based memristor. This is an important investigation and requires more comprehensive studies in the future work.

4. Conclusion

In summary, a memristor with active resistive switching layer formed by a honey film was fabricated and characterized. The device demonstrated bipolar resistive switching with a fast switching speed of 100 ns SET time and 500 ns RESET time, comparable with other reported resistive switching devices. The honey-based memristor successfully emulated STDP and SRDP, two important synaptic learning functions in biological neurons. The honey film was soluble in water, exhibiting biodegradability of the memristor. All these characteristics demonstrated the potential of honey-based memristive synaptic devices for energy efficient SNNs in biodegradable neuromorphic systems, which are promising to address the challenges of power consumption and electronic wastes faced by conventional Si-based computing systems.

Data availability statement

The data that support the findings of this study are available upon reasonable request from the authors.

Acknowledgment

Feng Zhao acknowledges the support from the National Science Foundation, United States (ECCS-2104976).

Conflict of interest

The authors declare that they have no known competing financial interests or personal relationships that could have appeared to influence the work reported in this paper.

ORCID iD

Feng Zhao https://orcid.org/0000-0001-9350-6497

References

[1] Ren Z Y, Zhu L Q, Guo Y B, Long T Y, Yu F, Xiao H and Lu H L 2020 *ACS Appl. Mater. Interfaces* **12** 7833
[2] Bi G and Poo M 2001 *Ann. Rev. Neurosci.* **24** 139
[3] Sjöström P J, Rancz E A, Roth A and Häusser M 2008 *Physiol. Rev.* **88** 769
[4] Panwar N, Rajendran B and Ganguly U 2017 *IEEE Electron Device Lett.* **38** 740
[5] Hebb D O 1949 *The Organization of Behavior: A Neurophysiological Approach* (New York: Wiley)
[6] Dang B J, Wu Q T, Song F, Sun J, Yang M, Ma X H, Wang H and Hao Y A 2018 *Nanoscale* **10** 20089
[7] Kim M and Lee J 2018 *ACS Nano* **12** 1680
[8] John R A, Ko J, Kulkarni M R, Tiwari N, Chien N A, Ing N G, Leong W L and Mathews N 2017 *Small* **13** 170119332
[9] Nishitani Y, Kaneko Y, Ueda M, Morie T and Fujii E 2012 *J. Appl. Phys.* **111** 124108
[10] Yang J T, Ge C, Du J Y, Huang H Y, He M, Wang C, Lu H B, Yang G Z and Jin K J 2018 *Adv. Mater.* **30** 1801548
[11] Chen F D *et al* 2021 *J. Mater. Chem.* C **9** 8372
[12] Zhu J D, Zhang T, Yang Y C and Huang R 2020 *Appl. Phys. Rev.* **7** 011312
[13] Wu G D, Feng P, Wan X, Zhu L Q, Shi Y and Wan Q 2016 *Sci. Rep.* **6** 23578
[14] Wu G D, Zhang J, Wan X, Yang Y and Jiang S H 2014 *J. Mater. Chem.* C **2** 6249
[15] Park Y J and Lee J-S 2017 *ACS Nano* **11** 8962
[16] Aleksey S, Xing Y, Cheong K Y, Zeng X Q and Zhao F 2020 *Mater. Lett.* **271** 127796
[17] Sueoka B, Cheong K Y and Zhao F 2021 *Mater. Lett.* **308** 131169
[18] Yoshida C, Tsunoda K, Noshiro H and Sugiyama Y 2007 *Appl. Phys. Lett.* **91** 223510
[19] Xu J Q, Zhao X N, Wang Z Q, Xu H Y, Hu J L, Ma J G and Liu Y C 2019 *Small* **15** 1803970
[20] Chen A, Haddad S, Wu Y C, Fang T N, Kaza S and Lan Z 2008 *Appl. Phys. Lett.* **92** 013503
[21] Gao S *et al* 2014 *Appl. Phys. Lett.* **105** 063504
[22] Mazur T, Zawal T and Szaciłowski K 2019 *Nanoscale* **11** 1080
[23] Bliss T V P and Collingridge G L 1993 *Nature* **361** 31
[24] Du C, Ma W, Chang T, Sheridan P and Lu W D 2015 *Adv. Funct. Mater.* **25** 4290
[25] Kandel E R and Schwartz J H 1985 *Principles of Neural Science* (Amsterdam: Elsevier) (https://doi.org/10.1126/science.3975635)
[26] Azghadi M R, Linares-Barranco B, Abbott D and Leong P H W 2017 *IEEE Trans. Biomed. Circuits Syst.* **11** 434
[27] Azghadi M R *et al* 2020 *Adv. Intel. Syst.* **2** 1900189
[28] Wu S W *et al* 2016 *IEEE Electron Device Lett.* **37** 990
[29] He X L, Zhang J, Wang W B, Xuan W P, Wang X Z, Zhang Q H, Smith C G and Luo J K 2016 *ACS Appl. Mater. Interfaces* **8** 10954
[30] Nyenke C and Dong L 2016 *Microelectron. Eng.* **164** 48